BARIUM IN TWILIGHT ZONE SUSPENDED MATTER AS A POTENTIAL PROXY FOR PARTICULATE ORGANIC CARBON REMINERALIZATION: RESULTS FOR THE NORTH PACIFIC

F. Dehairs[1], S. Jacquet[1], N. Savoye[1,*], B. A. S. Van Mooy[2], K.O. Buesseler[2], J.K.B. Bishop[3,4], C. H. Lamborg[2], M. Elskens[1], W. Baeyens[1], P.W. Boyd[5], K.L. Casciotti[2] and C. Monnin[6]

1. Department of Analytical and Environmental Chemistry, Vrije Universiteit Brussel, Pleinlaan 2, B-1050 Brussels, Belgium

2. Department of Marine Chemistry and Geochemistry, Woods Hole Oceanographic Institution, Massachusetts, 02543, USA

3. Lawrence Berkeley National Laboratory, 1 Cyclotron Road, Berkeley, CA 94720, USA

4. Department of Earth and Planetary Science, University of California – Berkeley, Berkeley, CA 94720

5. Centre for Chemical and Physical Oceanography, Department of Chemistry, PO Box 56, Dunedin, New Zealand

6. CNRS-Université Paul Sabatier, Laboratoire Mécanismes et Transferts en Géologie (LMTG), 14 avenue Edouard Belin, 31400 Toulouse, France

* Now at: Observatoire Aquitain des Sciences de l'Univers, UMR EPOC, CNRS / Université Bordeaux 1, Station Marine d'Arcachon, 2 rue du Pr. Jolyet, 33120 Arcachon, France

ABSTRACT

This study focuses on the fate of exported organic carbon in the twilight zone at two contrasting environments in the North Pacific: the oligotrophic ALOHA site (22°45' N 158°W; Hawaii; studied during June–July 2004) and the mesotrophic Subarctic Pacific K2 site (47°N, 161°W; studied during July-August 2005). Earlier work has shown that non-lithogenic, excess particulate Ba (Ba_{xs}) in the mesopelagic water column is a potential proxy of organic carbon remineralization. In general Ba_{xs} contents were significantly larger at K2 than at ALOHA. At ALOHA the Ba_{xs} profiles from repeated sampling (5 casts) showed remarkable consistency over a period of three weeks, suggesting that the system was close to being at steady state. In contrast, more variability was observed at K2 (6 casts sampled) reflecting the more dynamic physical and biological conditions prevailing in this environment. While for both sites Ba_{xs} concentrations increased with depth, at K2 a clear maximum was present between the base of the mixed layer at around 50m and 500m, reflecting production and release of Ba_{xs}. Larger mesopelagic Ba_{xs} contents and larger bacterial production in the twilight zone at the K2 site indicate that more material was exported from the upper mixed layer for bacterial degradation deeper, compared to the ALOHA site. Furthermore, application of a published transfer function (Dehairs et al., 1997) relating oxygen consumption to the observed Ba_{xs} data indicated that the latter were in good agreement with bacterial respiration, calculated from bacterial production. These results corroborate earlier findings highlighting the potential of Ba_{xs} as a proxy for organic carbon remineralization.

The range of POC remineralization rates calculated from twilight zone excess particulate Ba contents did also compare well with the depth dependent POC flux decrease as recorded by neutrally buoyant sediment traps, except in 1 case (out of 4). This discrepancy could indicate that differences in sinking velocities cause an

uncoupling of the processes occurring in the fine suspended particle pool from those affecting the larger particle pool which sustains the vertical flux, thus rendering comparison between both approaches risky.

INTRODUCTION

The oceanic biological pump controls export of carbon to the deep sea via the production of sinking particles. The efficiency of this mechanism for longer term sequestration of carbon in the ocean is largely set by the intensity of biological consumption and remineralization of organic carbon in the twilight zone (see Buesseler et al., 2007). Earlier work has shown that twilight zone accumulation of discrete micro-crystals of barite which originally precipitate inside micro-environments such as biogenic aggregates and pellets (Dehairs et al., 1980; Bishop, 1988; Tazaki et al., 1997; Ganeshram et al., 2003; Lam and Bishop, 2007) does reflect remineralization of exported organic matter (Dehairs et al., 1992; 1997; Cardinal et al., 2001, 2005; Jacquet et al., 2007a, b).

In the upper mixed layer particulate Ba occurs mostly as adsorbed or incorporated on organic matter, carbonate and celestite (see e.g. Dehairs et al., 1980; Collier et al., 1984; Jacquet et al., 2007b) and only a small fraction of total Ba is identifiable as barite crystals which, however, become the predominant Ba phase with increasing depth. The biogenic aggregate is considered a necessary substrate for barite formation because $BaSO_4$ saturation conditions might prevail inside these micro-environments (Bishop, 1988; Dehairs et al., 1980) in contrast to ambient seawater which largely remains undersaturated (Monnin et al., 1999; Monnin and Cividini, 2001). Formation of barite is likely a continuous process through the mesopelagic water column as indicated by the $^{228}Ra/^{226}Ra$ ratios in suspended matter which are close to those for ambient seawater, suggesting local formation of barite (van Beek et al., 2007). This authigenic formation of barite in the water column associated with the occurrence and processing of biogenic matter is reflected in the shape of the oceanic dissolved Ba profile. The latter is characteristic for a bio-intermediate element, showing moderate depletion in surface waters (see Chan et al; 1979; Broecker and Peng, 1982).

In the present work we compare the water column distribution of the Ba_{xs} proxy at two North Pacific sites (ALOHA, Hawaii and K2, south of Kamchatka) which differ strongly in terms of ecosystem functioning. We confront estimates of organic carbon remineralization obtained via the Ba_{xs} proxy approach with estimates of bacterial carbon respiration obtained from bacterial production and with POC flux attenuation obtained from neutrally buoyant sediment traps (NBST) deployed in the twilight zone. The overall aim is to constrain the twilight zone heterotrophic processing of organic carbon by comparing these three conceptually very different approaches.

This work is part of the VERTIGO (VERtical Transport In the Global Ocean) research project which focused on the processes controlling the efficiency of particle export between the surface and deep ocean (Buesseler et al., 2007). During VERTIGO several approaches to assess carbon export and remineralization were compared at two locations in the North Pacific contrasting in terms of particle flux magnitude, composition of sinking and suspended particles and remineralization length scales. We sampled the oligotrophic Hawaii Ocean Time series station ALOHA (22°45' N 158°W; see Karl and Lukas, 1996) during June–July 2004 and the High Nutrient Low Chlorophyll (HNLC) Japanese time series station K2 located near the centre of the Subarctic gyre (47°N, 161°W; Honda et al., 2006) during July-August 2005. The studies included new production (Elskens et al., this volume), particle flux assessment via neutrally buoyant sediment trap (NBST) devices (Stanley et al., 2004; Andrews et al., 2006; Buesseler et al., 2007; Lamborg et al., this volume), ^{234}Th deficit (Pike et al., 2006), phytoplankton composition (Silver et al., 2006) bacterial and zooplankton biomass and carbon demand (Wilson et al., this issue; Van Mooy et al., this issue; Steinberg et al., in press).

METHODS

Site descriptions

Occupation of the study sites was from June 22 to July 9, 2004, for ALOHA (22°45' N 158°W; Hawaii; R/V Kilo Moana), and from July 22 to August 18, 2005 for K2 (47°N; 161°W; R/V Roger Revelle). Over the period of study the ALOHA site remained confined inside an anticyclonic vortex. At K2 the upper 500m of the water column is influenced by the Oyashio current flowing in an easterly direction (Buesseler et al., this volume). The ALOHA and K2 sites contrast largely regarding the strength and source characteristics of the biological pump, characterized by carbonate and silicate predominance, respectively (Buesseler et al., 2007 and this volume). ALOHA is an oligotrophic site, characterized by low nutrient, low chlorophyll and low *f*-ratios (Karl et al., 1996). Coccolithophorids are common at the ALOHA site (e.g. Cortés et al., 2001) and material collected by the NBST's deployed at 150m, 300m and 500m is characterized by a relatively larger contribution of $CaCO_3$ as compared to K2 (Buesseler et al., 2007; Lamborg et al., this volume). The subarctic K2 site is characterized by high surface nutrients, including silica (Saito et al., 2002) and clear diatom dominance (Honda, 2003; Honda et al., 2006; Buesseler et al., this volume; Silver et al., 2006). As a result opal is the major constituent of the material trapped by the NBST's deployed at 150, 300 and 500m at K2 (Buesseler et al., 2007, Lamborg et al., this volume). New production estimates and export ratios at both sites indicate larger potential for export at K2 compared to ALOHA (Honda, 2003; Karl et al., 1996; Elskens et al., this volume). Bacteria and zooplankton biomasses were significantly higher at K2 than at ALOHA (Steinberg et al., in press; Van Mooy et al., this issue; Wilson et al., this issue).

Figure 1 shows the T-S diagrams for the upper 1000 m of water column at both study sites. Salient features at ALOHA are the thermocline region (= Eastern North Pacific Central Water; Tomczak and Godfrey, 1994) stretching between a shallow salinity

maximum (35.2 at about 150m) and a deep salinity minimum (34 at about 500m). The upper boundary of the seasonal thermocline at ALOHA is located between 36 and 62m (Figure 1C), while at K2, it is confined between 18 and 32m (Figure 1 C), indicating the upper mixed layer was slightly shallower at the latter site. Below the seasonal thermocline at K2 a clear temperature minimum (close to 1.45°C) is observed around 100m (Figure 1A), overlaying the Pacific Subarctic Water body (Tomczak and Godfrey, 1994). The latter shows a temperature maximum (3.4°C) around 300m above the oxygen minimum waters (O_2 25μM; Figure 1B). At the K2 site all T-S diagrams closely overlap except one cast, located at 46°N, 161°W, 1° south of the area at 47°N; 160°-161°W, where all 5 other casts were taken. This particular cast has a slightly different T-S profile with warmer temperature minimum waters (2.3°C) and higher oxygen contents in the subsurface (Figure 1B).

Suspended matter sampling and analysis

We sampled suspended matter from 5 casts at ALOHA (Julian days 178, 182, 186, 188, 191) and 6 casts at K2 (Julian days 209, 212, 214, 219, 223, 225) using a CTD rosette equipped with 10L Niskin bottles. Suspended matter was sampled at 14 depths between surface and 1000m. Between 3 and 10 L of seawater was filtered through 47mm diameter, 0.4μm pore size Nuclepore membranes, under pressure of filtered (0.4 μm) air.

The detailed procedure for suspended matter element analysis is given in Cardinal et al. (2001). Briefly, particulate material was completely digested in sealed Teflon beakers using a hot HF/HCl/HNO_3 mixture (1.5/1/0.5 ml). Analysis was done by Inductively Coupled Plasma – Atomic Emission Spectroscopy (ICP-AES, Thermo-Optics, IRIS) for Al and Inductively Coupled Plasma – Quadrupole Mass Spectrometry (ICP-QMS, VG Instruments, Plasma PQ2+) for Ba and Sr. Biogenic Ba (hereafter called excess Ba or Ba_{xs}) was calculated by subtracting the lithogenic Ba

from total Ba. Lithogenic Ba was estimated from the Al content and a Ba/Al molar ratio for the lithogenic component. We applied a value of 0.00073 for the Ba/Al molar ratio as reported for the lithogenic fraction of marine sediments (see Reitz et al., 2004). This ratio is about a factor 2 smaller than values for crustal ratio reported in the literature (e.g. Taylor and McLennan, 1985). Using either lithogenic reference has but a minimal impact on the calculations for twilight zone organic carbon processing.

Dissolved Ba sampling and analysis

15 ml of unfiltered seawater were sampled in polypropylene vials (Nalgene), rinsed three times with the seawater sample. Samples were acidified using Suprapur HCl (15 µl) and stored at room temperature till analysis. At ALOHA and K2 6 casts (0-1000m) were sampled during the site occupation. Dissolved barium was measured using an isotope dilution ICP-QMS (ID-ICP-QMS) as described by Klinkhammer and Chan (1990) and Freydier et al. (1995). Sample preparation is as follows: 1 g of seawater is spiked with 0.7 g of ^{135}Ba-spike solution yielding a ^{138}Ba/^{135}Ba ratio between 0.7 and 1 to minimize error propagation [Webster, 1960; Klinkenberg et al., 1996]. Subsequently the sample is diluted with Milli-Q grade water to a final weight of 30 g. Blanks consist of acidified (nitric acid) Milli-Q water. Quantities of sample, spike and dilution water were accurately assessed by weighing.

Isotope ratios were measured with a SF-ICP-MS (Element 2 Thermo Finnigan). Reproducibility of our method is ± 1.5% (RSD) as tested on repeat preparations of reference solutions. Average Ba values obtained for reference waters SLRS-3 and an in house standard (i.e. a Mediterranean Sea standard prepared by C. Jeandel, OMP, Toulouse) were 13.48 ± 0.21 µg l^{-1} (1σ) with RSD of 1.55% and 10.49 ± 0.29 µg l^{-1} (1σ) with RSD of 2.75% respectively, in good agreement with certified values (SLRS-3: 13.4 ± 0.6 µg l^{-1} and OMP: 10.4 ± 0.2 µg l^{-1}). For the ALOHA site characterized by

very stable hydrographic conditions over the duration of the investigation, overall precision (including sampling precision) based on the 6 dissolved Ba profiles is ± 0.3 $\mu g\ l^{-1}$ (1σ) with an RSD of 5%.

Bacterial production, carbon demand and respiration

Bacterial production (BP) was determined using [methyl-^{3}H]-thymidine (TdR) incorporation incubations conducted at one atmosphere pressure and *in situ* temperatures (Fuhrmann and Azam, 1982). Triplicate, acid-washed, 30 mL polycarbonate bottles were filled with seawater from each depth and spiked with 20 nmol L^{-1} of [methyl 3H] thymidine. Replicate incubations were poisoned with 3% formaldehyde (final concentration) prior to addition of the methyl-^{3}H thymidine. All bottles were incubated for 24 hours. TdR incorporation rates were determined following trichloroacetic acid precipitation and filtration as described by Carlson et al (1996). BP was calculated from TdR incorporation rates using TdR conversion factors of 1 - 2 x 10^{18} cells mol^{-1} and a carbon conversion factor of 15 fg C $cell^{-1}$; these values approximate the median of those published for bacterial communities in surface waters (see Ducklow, 2000 and references therein; Steinberg et al., in press). Bacterial respiration (BR) was calculated assuming that bacterial growth efficiency (BGE) ranged between 0.10 and 0.15 (see discussion by del Giorgio and Cole, 2000); this range was derived from nearly two dozen published values for surface bacterial communities. Bacterial respiration (BR) was calculated as the quotient of BP and BGE, minus BP (BR = (BP/BGE) - BP). The purpose of adopting a range in conversion factors and BGE values is to calculate different values of bacterial respiration (BR) at each depth in an attempt to faithfully constrain the uncertainty in these unknown parameters.

RESULTS

Excess, non-lithogenic Ba

For the upper 120m waters at ALOHA, which are very low in total Ba, non-lithogenic Ba fractions ranged between 68 and 98%, with a single surface water sample (25m) showing 100% lithogenic Ba. For all other depths at ALOHA the non-lithogenic Ba fraction was > 91%. At K2 non-lithogenic Ba was consistently > 91%, except one case at 25m where it reached only 73%. Thus, overall most of particulate Ba is associated with non-lithogenic matter and results from biogeochemical processes in the water column; this fraction is called hereafter excess-Ba or Ba_{xs}. Previous work in different oceanic environments showed that Ba_{xs} below the upper mixed layer mainly consists of micron sized discrete barite particles, while within the upper mixed layer other biogenic carriers (celestite, carbonate and detrital organic matter) may account for a significant fraction of Ba_{xs} (Dehairs et al., 1980; Stroobants et al., 1991; Sternberg, 2005; Jacquet et al., 2007b). Therefore, it is most likely that for the subsurface and mesopelagic domain at ALOHA and K2, micron-sized crystalline barite is the main Ba carrier as well.

Particulate excess Ba profiles

Surface waters (<150m) at both ALOHA and K2 sites are very low in Ba_{xs} (<50 pM) what contrasts with observations for the Southern Ocean where occasionally very high values, even exceeding 1000 pM, have been reported for the surface mixed layer (Dehairs et al., 1997; Cardinal et al., 2001; Jacquet et al., 2005) and which in at least one situation was associated with presence of large numbers of $SrSO_4$ secreting acantharians (Jacquet et al., 2007b).

At station K2 Ba_{xs} profiles show a large variability (Figures 2C,D and 3A) in agreement with more dynamic conditions of water mass circulation and ecosystem functioning prevailing at K2 (Buesseler et al., this volume). This increased variability, however, does not obscure the clear pattern emerging from the average profile as shown in Figure 3A. Ba_{xs} contents sharply increase with depth, contrasting with the more gradual increase observed at ALOHA. A first shallow Ba_{xs} maximum of 420 pM is reached between 55 and 80m coinciding quite well with the deep Chl-a maximum located at 50 to 60m, just underneath the seasonal thermocline (Buesseler et al., this volume). A second larger maximum of 505 pM is reached around 200m, within the strong oxygen gradient (compare Figures 1B and 3A). Figure 3A also shows that the shallow and deeper Ba_{xs} maxima are nicely coincide also with maxima of particulate ^{234}Th which reflect significant local accumulation of particles that scavenged ^{234}Th from solution (data from Buesseler et al., in preparation for second DSR II volume). Furthermore, Lam and Bishop observe maxima of particulate Fe, Mn occur at slightly shallower depths than the Ba_{xs} maximum discussed here (Lam and Bishop, submitted). The latter authors take these subsurface Fe and Mn peaks to reflect advection of resuspended matter from the Kuril Kamchatka island-arc sill as is suggested also by the work of Nishioka et al. (2007). This raises the question whether also Ba_{xs} could be partly affected by advection. At depths >300m, average Ba_{xs} contents at K2 decrease again to range between 230 and 280 pM. At 1000m, the deepest depth sampled, Ba_{xs} increases again to 380 pM (Figure 3A).

At ALOHA Ba_{xs} concentrations increase with depth from about 30 pM in the upper 100m and remain uniform around 230 pM between 400 and 1000m. The variability of the Ba_{xs} contents for successive casts over 3 weeks time is remarkably small at ALOHA with relative standard deviation values for depths >200m being 17% on average (Figure 3A. Over the period of study the ALOHA site remained confined

inside an anticyclonic vortex (Buesseler et al., this volume), a condition which probably contributed to maintaining relatively stable production and export regimes.

At K2 Ba_{xs} contents increased significantly by about 50% (t-test; $p<0.05$) between the first and second NBST deployment (Figure 2 C,D). This increase is mainly due, however, to the high Ba_{xs} concentrations of cast 72 which also exhibits high Al values (Figure 2B), possibly indicating advection (see further, discussion section). Without considering the cast 72 data the Ba_{xs} increase during the K2 station occupation appears not to be significant (t-test; $p>0.05$).

Overall, the contrasting Ba_{xs} contents in subsurface and mesopelagic waters between ALOHA and K2 likely reflect differences in export and remineralisation regimes between both environments.

Particulate Sr and Al profiles

Other studies have assessed the Ba-barite content from discrete barite particle counting and sizing (see Dehairs et al.1980; Stroobants et al., 1989; Robin et al., 2003; Jacquet et al., 2007b). Besides barite, celestite ($SrSO_4$) synthesised by acantharians can be a significant contributor to Ba_{xs} (Bernstein et al., 1998; Bernstein and Byrne, 2004, 1998; Jacquet et al., 2007b). To get an insight in the possible contribution of celestite to the Ba_{xs} content, particulate Sr contents were assessed and associated Ba contents estimated (see further below).

In contrast to Ba_{xs}, particulate Sr contents are highest in the upper 80m. At ALOHA averaged Sr contents reach up to 960 pM and decrease with depth to values <300 pM (Figure 3B). A second, smaller Sr peak of 520 pM occurs at 320m.

At K2 surface water Sr values are much lower than at ALOHA, with a Sr peak value at 30m not exceeding 330 pM. The overall relatively low particulate Sr content at ALOHA and K2 (<1 nM), compared to the 10 times higher concentrations during a

situation with abundant acantharians (Southern Ocean EIFEX cruise; Jacquet et al., 2007b), suggests that acantharians were not present in large numbers at the North Pacific sites studied here.

By applying a Ba/Sr molar ratio of $2.6x10^{-3}$ for acantharians (Bernstein et al., 1998) and assuming that all Sr is associated with acantharian celestite, we calculate for the upper 150m, where Sr contents are highest, that 1.2% and 7.4% of excess Ba could be contributed by acantharians at K2 and ALOHA, respectively. In the twilight zone and at greater depths this fraction is <1%. This highlights the peculiar condition of Ba_{xs} which in essence is not present as a minor component in other biogenic phases such as carbonate and celestite, but is most likely present essentially as microcrystalline barite as was observed for other oceanic systems.

Al informs not only on the lithogenic component of suspended matter, but also on the presence of material possibly advected from nearby margins. Al contents at ALOHA (data not shown) show an average water column content around 6 nM (not including a single high of 25 nM at 25m), with concentrations at depths >400m, slightly exceeding those in the <400m part of the water column. At K2, Al values are low (<4 nM) in the upper 50m but increase to values ranging between 5 and 27 nM between 80 and 800m (see Figure 2A,B). One profile (cast 72) shows higher Al contents (up to 50 nM) in the upper 600m and largely accounts for the 47% increase of the Al content in the upper 600m during the second half of the K2 study period. Although Ba_{xs} contents as well increase during the second half of the K2 study period, the overall correlation between Al and Ba_{xs} is weak ($r^2 = 0.38$; $p<0.05$), suggesting the distributions of these two elements are mostly governed by different processes. Overall, at K2 particulate Al and Ba_{xs} contents in the upper 400m exceed those at ALOHA by about a factor 2 and 3, respectively.

DISCUSSION

Comparing subsurface and mesopelagic Ba_{xs} contents at ALOHA and K2

Figure 3A illustrates the large differences in concentrations and profile shapes between ALOHA and K2 sites, which are particularly salient in the subsurface and mesopelagic waters. The upper 1000m Ba_{xs} signal is low and stable over time at ALOHA, while at K2 signals are larger but more variable (Figure 2C,D). It is unlikely that this variability is due to changing water masses since all casts sampled for Ba_{xs} (except one cast at 46°N showing slightly warmer temperature minimum water and higher O_2 contents; see section Site descriptions in Methods) show near identical T-S plots. Considering that the mesopelagic Ba_{xs} signal is related with degradation of organic matter (Dehairs et al., 1992; 1997) our data indicate more intense production, export and processing of exported organic material in the HNLC Subarctic Pacific as compared to the oligotrophic subtropical ALOHA site. This is in agreement with significantly higher biomasses, productivities and POC export fluxes reported for K2 (Buesseler et al., 2007; Boyd et al., this volume; Elskens et al., this volume).

The occurrence of two Ba_{xs} maxima at K2 is striking (a first small peak between 50 and 80m and a second larger peak between 200 and 300m). The shallowest Ba_{xs} peak, underneath the upper mixed layer, underlays the deep chlorophyll maximum and coincides with a shallow ^{234}Th peak (Buesseler et al. this volume and in preparation for DSR II vol. 2, and see Figure 3A). By comparing nitrogen nutrient drawdown budgets from the upper mixed layer with the 150m neutrally buoyant sediment trap N-fluxes, Buesseler et al. (this volume) conclude that significant remineralization takes place between 50 and 150 m. This is the depth layer where the first Ba_{xs} peak is located, and might indicate a relationship between Ba_{xs} and remineralization as observed elsewhere for the deeper mesopelagic Ba_{xs} peak (Dehairs et al., 1997;

Cardinal et al., 2005; Jacquet et al., 2007a). The occurrence of marine snow at the base of the mixed layer, as reported in other studies (e.g. Lampitt et al., 1993) would offer an appropriate substrate for Ba_{xs} formation, giving rise to the Ba – barite enrichments in the larger (> 53 μm) particle size fraction reported by Bishop (1988). The presence here of a Ba_{xs} maximum just below a quite shallow upper mixed layer (~50m) is nevertheless peculiar and has not been observed in our Southern Ocean studies, where shallow peaks of Ba_{xs} do occasionally occur within the mixed layer and usually coincide with significantly increased biogenic silica or celestite (Dehairs et al. 1997; Cardinal et al., 2001, 2005; Jacquet et al., 2007b).

The second deeper Ba_{xs} maximum at 200-300m (Figures 2B,D and 3A) again coincides with a particulate ^{234}Th maximum and in 2 cases out of 6 (casts 50 and 72) with an Al maximum (compare Figures 2 B and 2D). Though advection of predominantly redox sourced particulate Fe and Mn from the margins to the west reported by Lam and Bishop for this same expedition (Lam and Bishop, in review) is in agreement with such occasional co-variation between Al and Ba_{xs}, overall, however, the correlation between Al and Ba_{xs} at K2 is weak (see results section). Therefore, other processes could be operating, such as: scavenging of fine clay particles and associated elements by aggregates (e.g. Alldredge and Silver, 1988; Passow et al., 2001) as well as incorporation of such finer particles into fecal pellets and adsorption of dissolved Al on sinking particles (Murray and Leinen, 1996; Kryc et al., 2003). These combined processes could represent a mechanism inducing correlative behaviour between biogenic and lithogenic elements. In addition, at K2, zooplankton activity, in particular, could represent a further important mechanism conducive to the observed correlations via the injection at depth of particles (biogenic and lithogenic) previously scavenged from surface waters during grazing activity. Indeed Steinberg et al. (in press) report the consistent presence of increased

zooplankton biomass (>335 μm; with copepods representing 67% of total abundance) in the 200 to 450m depth layer at K2, with evidence of day-night migration between these depths and the upper mixed layer.

Ba_{xs} contents and bacterial activity

Prior work identified the biogenic micro-environment (aggregates, pellets) which are subject to bacterial degradation as the sites of barite formation (Dehairs et al., 1980; Bishop, 1988; Dehairs et al., 2000; Ganeshram et al., 2003). Furthermore, a direct link between bacterial activity and barite formation is evidenced by Gonzalez-Muñoz et al. (2003) based on work with bacterial cultures grown on Ba enriched substrate. Recent results for the Kerguelen Plateau area in the Southern Ocean also highlight the relationship between bacterial activity and barite (measured as Ba_{xs}) in suspended matter (Jacquet et al., in press). Prior to comparing mesopelagic Ba_{xs} contents and bacterial activity we briefly discuss the choice of conversion factors used to calculate bacterial production (BP) and bacterial respiration (BR).

It is likely that the conversion factors used to calculate BP from [methyl-^{3}H]-thymidine (TdR) incorporation rates varied between ALOHA and K2 and also with depth at these two locations. It is also likely that the BGE values used to calculate BR from BP also varied. We used a range in these values in order to constrain much of the geographic variability observed in the open ocean (see discussion of Ducklow, 2000; del Giorgio and Cole, 2000). While the influence of pressure on conversion factors used to transform TdR incorporation rates to BP has yet to be systematically examined, we know of no *a priori* reason to expect that they should vary with depth and conversion factors for surface communities have been applied previously to the mesopelagic (e.g Nagata et al., 2000; Tamburini et al., 2002; Reinthaler et al., 2006; Steinberg et al., in press). However, the TdR incorporation rates derived from

incubations conducted at atmospheric pressure may underestimate true rates (Bianchi et al., 1999; Eardly et al., 2001; Tamburini et al., 2002; Turley and Dixon, 2002) and, thus, the BP rates we present here are conservative. The impact of pressure on BGE is also uncertain, and our range of values accounts for this to a certain degree. Nagata et al (2000) applied a BGE of value of 0.20 in their study of bathypelagic (> 100 m depth) bacterial communities. However, Reinthaler et al (2006) recently reported that BGE was significantly lower (0.01 - 0.03) for several bathypelagic communities as well as two communities within the mesopelagic. As with our study, their incubations were conducted on a research vessel at one atmosphere, and thus do not account for the effects of decompression. Tamburini et al (2003) reported that decompressed communities may operate at lower BGE's at one atmosphere than under in situ pressures, and thus the values of Reinthaler et al (2006) might represent a lower limit for BGE. Given that the variability of BGE with depth remains fairly uncertain and that our study focuses primarily on depths less than 500m, we posit that our range of 0.10 - 0.15 allows a reasonable estimate of BR. Clearly if BGE values are ultimately found to fall outside this range, our analysis of the relationship between Ba_{xs} and BR will need to be revisited. Results for bacterial production (BP) and bacterial respiration rate (BR) shown here are also discussed in Steinberg et al. (in press).

For comparison with Ba_{xs} we will only consider bacterial production data for casts reaching 1000m, i.e. the deepest depth sampled for Ba_{xs}. Column integrated (0-1000m) BP values are not very different between ALOHA and K2 sites (overall range is between 69 and 98 mg C m^{-2} d^{-1}). However, there is a clear difference between both sites in terms of surface to deep gradients in BP. At ALOHA this gradient is steep (Figure 4) with only 16% of the 1000m column integrated BP occurring below 100m, in the mesopelagic (thus indicating that most of the bacterial production is confined

within the upper 100m), while at K2 column integrated BP below 100m represents 33% of the 1000m column integrated value.

In the following we focus specifically on the 150 to 500m depth interval where the K2 mesopelagic Ba_{xs} maximum is located and where the NBST's were deployed (Buesseler et al., 2007). In Figure 5 and Table 1 we compare column integrated bacterial activity and average Ba_{xs} contents for the 150 to 500m depth interval at ALOHA and K2 for casts sampled close by in time. It is clear that the larger mesopelagic Ba_{xs} contents at K2 coincide with larger column integrated bacterial activities. We will now assess the organic carbon remineralization rates reflected by the mesopelagic Ba_{xs} contents.

During earlier work on the Southern Ocean we proposed a simple relationship between mesopelagic Ba_{xs} and the rate of oxygen consumption as deduced from a 1D advection-diffusion model applied on highly resolved oxygen profiles (Shopova et al., 1995; Dehairs et al., 1997). It is tempting to compare the outcome of that Southern Ocean relationship, as applied to mesopelagic Ba_{xs} contents at ALOHA and K2, with the bacterial respiration rates at both sites. The transfer function proposed by Shopova et al. (1995) and Dehairs et al. (1997) is:

$$J_{O_2} = (mesoBa_{xs} - Ba_{residual}) / 17450 \qquad \text{eq.1}$$

$$C_{respired} = Z \times J_{O_2} \times RR \qquad \text{eq.2}$$

where JO_2 is the O_2 consumption (µmol l^{-1} d^{-1}), $C_{respired}$ is the mineralization rate of organic carbon (in mmol C m^{-2} d^{-1}), Z is the thickness of the mesopelagic layer, RR is the Redfield C/O_2 mole ratio (127/175; Broecker et al., 1985), meso-Ba_{xs} is the Ba_{xs} amount that accumulates over the growth season in the mesopelagic waters and $Ba_{residual}$ is the residual Ba_{xs} signal at zero oxygen consumption, i.e. at zero organic C respiration. This residual Ba_{xs} can be considered as 'preformed' Ba_{xs}, left-over after partial dissolution and sedimentation of Ba_{xs} produced during a previous

phytoplankton growth event. It is probable that the deduced O_2 consumption rate actually reflects combined bacterial and zooplankton respiration. The relative standard error associated with the calculations based on Eq. (1) ranges between 14 and 44%, and is on average 22%.

The fate of barite particles once freed from their protecting micro-environment envelope into the ambient seawater will depend on the $BaSO_4$ saturation state of the ambient seawater. In the Southern Ocean system for which eq. 1 was established, the water column is at equilibrium with $BaSO_4$ from the surface down to about 2000m (Monnin et al., 1999, 2006). For these waters the Ba_{xs} residual is estimated at 180 pM (Dehairs et al., 1997). In order to evaluate the potential for barite preservation once released in the water column for the North Pacific ALOHA and K2 sites, we need to check the degree of $BaSO_4$ saturation of the water column as this will affect the value of the residual Ba content, which is required to solve eq. 1. At ALOHA measured dissolved Ba concentrations increase regularly from a value of 30nM in surface waters to 137 nM at 3000 m, while at K2 this increase is from 65 nM in the surface to 97 nM at 2000m (Figure 6). Note that Ba content for the mesopelagic depth range at ALOHA is about half that at K2. Based on dissolved Ba content, temperature, depth and salinity, we calculated the barite saturation indices (Ω) for pure $BaSO_4$ and for Sr-substituted barites following the procedures described by Monnin et al. (1999) and Monnin and Cividini (2006). As previously found (Monnin and Cividini, 2006) the saturation states of the ALOHA and K2 waters with respect to pure $BaSO_4$ and Sr-substituted barites are similar. Equilibrium is reached at a depth of about 300 m at K2, while at ALOHA it is reached only below 1000 m. Significant undersaturation of ALOHA mesopelagic waters is indicated by a saturation index between 0.2 and 0.4.

For K2 the application of a transfer function originally elaborated for Southern Ocean conditions seems warranted since both systems have diatoms as a dominant

component of the phytoplankton community (North Pacific: see Honda et al., 2006; Buesseler et al, this volume; Southern Ocean: see e.g. Bathmann et al., 1997; Kopczynska et al., 2001) and since water temperatures in the mesopelagic layer are similar (typically ranging between 1.5 and 3.4°C; North Pacific: Buesseler et al., this volume, b; Southern Ocean: see Webb et al., 1991). ALOHA of course is quite different with higher temperatures, a larger temperature gradient through the upper mesopelagic (typically 8 to 22°C; Buesseler et al., this volume), and hosting a quite different algal community, with diatoms present but dominated by nano and picoplankton and including nitrogen fixers. However, considering that formation of excess Ba - barite in the water column is occurring throughout the World Ocean (Bishop, 1988; Dehairs et al., 1980; 1997; Bertram and Cowen, 1997; Cardinal et al., 2006) in situations with different plankton community regimes, we will assume as a first order approximation that the Southern Ocean transfer function relating mesopelagic Ba_{xs} content with oxygen consumption applies for this sub-tropical North Pacific environment.

To account for the state of $BaSO_4$ undersaturation in mesopelagic waters at ALOHA (Figure 6) we calculated JO_2 via eq. (1) but considered lower residual Ba_{xs} contents, which were assumed to range from 0 to 90 pM. At K2 the upper 300 m of water column are closer to $BaSO_4$ saturation but still undersaturated while below 300m waters are saturated. This condition was taken into account by assuming the residual Ba_{xs} content to range between 90 and 180pM. Table 1 compares calculations of bacterial respiration with carbon remineralization based on mesopelagic Ba_{xs} contents. Note that for K2, deep casts for BP (1000m) were taken only during the second NBST deployment. It appears that both approaches converge quite well and yield similar magnitudes of carbon remineralisation. Even considering that organic carbon remineralization calculated from mesopelagic Ba_{xs} would reflect combined bacterial

and zooplankton respiration, convergence of both approaches still holds. The maximum value of POC remineralisation based on Ba_{xs} at K2 would reduce from 106 to 55 mgC m^{-2} d^{-1} when the cast 72 data are omitted, considering that the high Al contents there might indicate advective input also of Ba_{xs} (see discussion above). In this case the Ba_{xs} based respiration rates are closer to the lower limit of the bacterial respiration rates (Table 1).

Overall the similarity in organic carbon respiration rates obtained from mesopelagic BP and Ba_{xs} contents is remarkable considering the uncertainty on the different conversion factors utilized in both calculations. This highlights an apparent relationship between bacterial activity and accumulation of Ba_{xs} in the twilight zone, which was suspected in earlier work. Future research should concentrate on this relationship to verify its robustness and possible generic character.

Mesopelagic Ba_{xs} and NBST POC fluxes

Neutrally buoyant sediment traps (NBST) were used to collect the sinking particle flux. These traps are subject to Lagrangian drifting and are designed to optimize particle capture in a fluid moving several orders of magnitude faster laterally (km d^{-1}) than mean particle sinking rates (10 to 100 m d^{-1}) (Buesseler et al., 2000; 2007).

Based on the POC fluxes recorded by the NBST's Buesseler et al. (2007) report lower transfer efficiencies (i.e. the ratio of the 500m POC flux over the 150m POC flux) at ALOHA as compared to K2. This condition is reflected by a larger 'Martin-curve' b-value (Martin et al., 1987) of 1.3 at ALOHA compared to a value of 0.5 at K2 (Buesseler et al., 2007). Higher b-values at ALOHA reflect the fact that the combined microbial and zooplankton communities there are tuned for rapid turn-over of the exported material, leaving little material for deep export and resulting in a short remineralization length scale. The system at K2 appears less efficient in retaining

organic matter in the mesopelagic waters, allowing for a larger fraction of the production to be exported below 500m, thereby increasing the mineralization length scale. When comparing mesopelagic Ba_{xs} inventories (and the bacterial remineralization these reflect) with the NBST POC flux at 150m, which represents the export flux from the surface, we observe that Ba_{xs}-based remineralization is larger in relative terms at ALOHA (consistent with a high b-value of 1.3), while it is relatively smaller for the first NBST deployment at K2, again consistent with the a low b value (0.5) there (Table 2). Note however, that during the second NBST deployment at K2 this comparison does not hold (Table 2; see discussion below). In absolute terms, however, mesopelagic remineralization at K2 exceeds the one at ALOHA. An apparent less efficient mesopelagic remineralization at K2 relative to POC input from above (case of first NBST deployment) could be sustained, at least partly, by the reported diurnal migration of mesozooplankton between surface and mesopelagic depths and which represents an efficient vehicle of organic matter to the mesopelagic depths (Steinberg et al., in press). It can be expected that bacteria will adapt to this condition of food supply and will extend their activity deeper in the water column. This is emphasized here by the significantly larger mesopelagic Ba_{xs} inventories at K2 compared to ALOHA.

In Table 2 we also compare POC remineralization from depth weighted average mesopelagic Ba_{xs} in the 150 to 500m layer with NBST POC flux decreases between 150 and 500m. Mesopelagic POC remineralization based on Ba_{xs} is of the same magnitude as the NBST POC flux decreases, except for the second NBST deployment at K2, where it exceeds the latter by up to a factor 10. When omitting the data for cast 72 characterized by a high Al content, possibly indicating advection also of Ba_{xs}, the maximum value of Ba_{xs} based POC respiration decreases from 106 to 55 mgC m^{-2} d^{-1} what strongly reduces the discrepancy with the NBST flux decrease, but does not

resolve it. This inverse behaviour of mesopelagic Ba_{xs} contents and NBST POC fluxes at K2 is puzzling: NBST POC fluxes decreased over the study period, thereby following new production (NP decreased from 151 to 72 mgC m^{-2} d^{-1}; Elskens et al. this volume; Table 2) while Ba_{xs} contents increased. Earlier Southern Ocean work showed that mesopelagic processing of exported organic carbon as reflected by Ba_{xs}, has a phase lag relative to the upper ocean processes (Dehairs et al., 1997; Cardinal et al., 2001; 2005) and therefore we do not, a priori, expect mesopelagic Ba_{xs} to be in phase with changes in surface water biomass and production.

We now investigate some scenarios offering a possible explanation for the discrepancies between POC flux decrease from traps and bacterial respiration.

Between both NBST deployments at K2 the contribution of larger phytoplankton (>20μm) to primary production decreased from 30 to 19% (Boyd et al., this volume) possibly inducing the observed decrease of POC flux during the second NBST deployment. We are uncertain whether this same condition of increased contribution of smaller sized phytoplankton to primary production would have inversely affected the mesopelagic Ba_{xs} stock. It is likely though that decreased phytoplankton cell sizes would rather favor water column organic matter accumulation as opposed to sinking, thereby enhancing mesopelagic remineralization and yielding increased Ba_{xs} contents.

However, the fact that flux attenuation for both NBST deployments at K2 is similar and even slightly less during the second NBST deployment at K2 (55% and 46% for deployment 1 and 2, respectively; Buesseler et al., 2007), speaks against enhanced remineralization during the 2nd NBST deployment. We notice furthermore that mesopelagic Ba_{xs} contents relate positively with the 500m POC fluxes normalized to the 150m POC fluxes, including the 2nd NBST trap data at K2 (from Table 2), in contrast with the comparison based on absolute POC flux values discussed above. When strictly adhering to a 1D view of the system's operation at K2, this would

suggest mesopelagic Ba_{xs} to be related with the ecosystem's characteristics such as for instance trophic structure and relative importance of the microbial loop, and not necessarily with magnitude of contemporaneous carbon export flux (which is smaller during the second NBST deployment at K2). However, the possibility that advection of fine particles in the mesopelagic layer could offset fluxes related to water column stocks from fluxes carried by sinking particles and recorded by the traps, can not be dismissed. As such, the different particulate carbon fluxes in the mesopelagic could be sustained by basically two different categories of particles:

(1) A category of particles consisting of large and fast sinking aggregates such as fecal pellets which are dependent on the activity of zooplankton in the trophic web (a condition that did remain relatively constant between NBST deployment 1 & 2 at K2; Steinberg et al., in press), and which sustain a POC attenuation profile that is rather independent of export magnitude (b-values don't change over time). Results for IRS traps (see Peterson et al., 2005 for IRS trap description) indicate that up to 70% of the POC flux at K2 was carried by fast sinking particles (sinking speeds exceeding 105m d^{-1}; Trull et al., this volume), emphasizing the significance of this category of particles in controlling the vertical POC flux;

(2) A second category consisting of smaller phytoplankton cells not selected for by the grazers and forming smaller and less densely packed aggregates which sink more slowly than fecal pellets and would be prone also to advective transport. Though barite has been identified inside large sized fecal pellets (Dehairs et al., 2000) we expect that the major loci of barite formation rather are less dense and more slowly sinking aggregates (Stroobants et al., 1990).

At this point no fully satisfactory explanation can be offered accounting for the discrepancies between Ba_{xs} based mesopelagic remineralization and POC flux decrease, as is especially salient for the second deployment at K2. However, if indeed

water column processing of finer particles is decoupled from processes acting on fast sinking particles, comparison between fluxes derived from water column Ba_{xs} stocks with fluxes sampled by sediment traps would not be meaningful. This would also imply that the similarity between trap measured POC flux decrease and Ba_{xs}-based remineralization observed for ALOHA and the first deployment at K2 is fortuitous.

CONCLUSIONS

This work investigated particulate Ba contents in the upper 1000m of the water column at two North Pacific sites (the oligotrophic ALOHA and the HNLC K2 time series sites) which contrast strongly in terms of carbon production and export. It appears that the vertical distributions of particulate non-lithogenic Ba (i.e. excess Ba or Ba_{xs}) in the water column also are quite different with higher mesopelagic Ba_{xs} contents at the more productive K2 site which also supports higher organic carbon export. We observed mesopelagic Ba_{xs} contents to closely follow trends in bacterial activity. Carbon respiration rates estimated using an empirical transfer function relating Ba_{xs} contents and oxygen consumption, established in earlier work, converge quite well with estimates based on bacterial production. While several questions, such as the assumed generic character of the Ba_{xs} based transfer function and the validity of the applied bacterial growth efficiencies, require further investigation, these results offer prospects for better constraining remineralization of particulate organic matter exported to the twilight zone, using the Ba_{xs} proxy.

Differences in relative importance of bacterial production in the mesopelagic part of the water column between ALOHA and K2, (At K2 mesopelagic bacterial production represents a larger fraction of total water column integrated BP compared to ALOHA), next to the mass-effect of exported POC (which is larger at K2) and

possibly advection of matter, are responsible for the differences in mesopelagic Ba_{xs} contents between both sites. Especially at the Subarctic Pacific K2 site, the comparison between carbon fluxes based on water column fine particle stocks and biological activities on the one hand and carbon fluxes recorded by sediment traps on the other, suggest an uncoupling between both, with the former possibly also sensitive to advection of material from upstream areas and not only to export from local surface waters.

ACKNOWLEDGMENTS

We acknowledge the skillful assistance of captain and crew of R/V Kilo Moana and R/V Revelle during work at sea. We are grateful to Jacques Navez and Laurence Monin for their help during sample preparation and elemental analysis at MRAC in Tervuren. Jim Valdes, Steve Manganini, Devon Ruddick, and Chanda Bertrand were also key to the success of the NBST sampling program and Steve Pike for thorium-234 sampling and analyses. This research was supported by Federal Science Policy Office, Brussels through contracts EV/03/7A, SD/CA/03A, the Research Foundation Flanders through Grant G.0021.04 and Vrije Universiteit Brussel via Grant GOA22, as well as the U.S. National Science Foundation programs in Chemical and Biological Oceanography. Work reported here (JKBB) was further supported by the U.S. Department of Energy, Office of Science, Biological and Environmental Research Program under Contract No. DE-AC02-05CH11231.

REFERENCES

Alldredge, A.L., Silver, M.W., 1988. Characteristics, dynamics and significance of marine snow. Progress in Oceanography, 20, 41-82.

Andrews III, J.E, Lamborg, C.H, Pike S, Steinberg, D, Wilson, S, Valdes, J, Buesseler, K.O., 2006. An examination of sediment trap accuracy issues during VERTIGO, 2006 Ocean Sciences, Honolulu, Hawaii.

Bathmann, U.V., Scharek, R., Klaas, C., Dubischar, C.D., Smetacek, V., 1997. Spring development of phytoplankton biomass and composition in major water masses of the Atlantic sector of the Southern Ocean. Deep-Sea Research II, 44, 51-67.

Bernstein, R.E., Byrne, R.H., Schijf, J., 1998. Acantharians: a missing link in the oceanic biogeochemistry of barium. Deep Sea Research, Part I, 45, 491– 505.

Bernstein, R.E., Byrne, R.H., 2004. Acantharians and marine barite. Marine Chemistry, 68, 45– 50.

Bertram, M. A. and J. P. Cowen, 1997. Morphological composition evidence for biotic precipitation of marine barite, Journal of Marine Research, 55, 577– 593.

Bianchi, A., Garcin, J., Tholosan, O., 1999. A high-pressure serial sampler to measure microbial activity in the deep sea. Deep Sea Research I, 46**:** 2129-2142.

Bishop, J.K.B., 1988. The barite - opal - organic carbon association in oceanic particulate matter. Nature, 332, 341-343.

Bishop, J.K.B., Schupack, D., Sherrell, R.M., Conte, M., 1985. A multiple unit large volume in situ filtration system (MULVFS) for sampling oceanic particulate matter in mesoscale environments. In: Zirino, A. (Ed.) Mapping Strategies in Chemical Oceanography, Advances in Chemistry Series, Vol. 209. American Chemical Society, Washington, DC, pp. 155-175.

Bishop J.K.B., 1989. Regional extremes in particulate matter composition and flux: Effects on the chemistry of the ocean interior, In: *Productivity of the Ocean:*

Present and Past, eds. W.H. Berger, V.S. Smetacek and G. Wefer, Willey & Sons Ltd, pp 117-137.

Boyd, P.W., Gall, M.P., Silver, M., Quantifying the surface-subsurface biogeochemical coupling during the VERTIGO HOT and K2 experiments, this issue.

Broecker, W.S., Peng, T.-H., 1982. Tracers in the Sea, Eldigio Press, 690pp.

Broecker, W.S., Takahashi, T., Takahashi, T., 1985. Sources and flow patterns of deep ocean waters as deduced from potential temperature, salinity and initial phosphate concentrations. Journal of Geophysical Research, 90, 6925-6939.

Buesseler, K.O., Lamborg, C.H., Boyd, P.W., Lam, P.J., Trull, T.W., Bidigare, R.R., Bishop, J.K.B., Casciotti, K.L., Dehairs, F., Elskens, M., Honda, M., Karl, D.M., Siegel, D., Silver, M.W., Steinberg, D.K., Valdes, J., Van Mooy, B., Wilson, S., 2007. Revisiting carbon flux through the ocean's twilight zone. Science, 316, 567-570.

Buesseler K. O., Steinberg D. K., Michaels A. F., Johnson R. J., Andrews J. E., Valdes J. R. and Price J. F., 2000. A comparison of the quantity and composition of material caught in a neutrally buoyant versus surface-tethered sediment trap, Deep Sea Research, I, 47, 277-294.

Buesseler, K.O., Trull, T.W., Steinberg, D.K., Silver, M.W., Siegel, D.A., Saitoh, S.-I., Lamborg, C.H., Lam, P.J., Karl, D.M., Jiao, N.Z., Honda, M.C., Elskens, M., Dehairs, F., Brown, S.L., Boyd, P.W., Bishop, J.K.B., Bidigare, R.R. .VERTIGO (VERtical Transport In the Global Ocean): a study of particle sources and flux attenuation in the North Pacific, this volume.

Cardinal, D., Dehairs, F., Cattaldo, T., André, L., 2001. Geochemistry of suspended particles in the Subantarctic and Polar front Zones south of Australia: Constraints

on export and advection processes. Journal of Geophysical Research, Oceans, 106, 31,637-31,656.

Cardinal, D., Savoye, N., Trull, T.W., André, L., Kopczynska, E. E., Dehairs, F., 2005. Variations of carbon remineralisation in the Southern Ocean illustrated by the Ba_{xs} proxy. Deep-Sea Research I, 52, 355-370.

Carlson, C. A., Ducklow, H. W., Sleeter, T. D., 1996. Stocks and dynamics of bacterioplankton in the northwestern Sargasso Sea. Deep Sea Research, II, 43, 491-515.

Chan L.H., Drummond, D., Edmond, J.M., Grant B., 1977. Barium Data from Atlantic GEOSECS Expedition. Deep-Sea Research, 24, 613-649.

Collier, R., Edmond, J., 1984. The trace element geochemistry of marine biogenic particulate matter. Progress in Oceanography, 13, 113-199.

Cortés, M.Y., Bollmann, J., Thierstein, H.R., 2001.Coccolithophore ecology at the HOT station ALOHA, Hawaii. Deep-Sea Research II, 48, 1957-1981.

Dehairs, F., Baeyens, W., Goeyens, L., 1992. Accumulation of suspended barite at mesopelagic depths and export production in the Southern Ocean. Science, 258, 1332 - 1335.

Dehairs, F., Chesselet, R., Jedwab, J., 1980. Discrete suspended particles of barite and the barium cycle in the open Ocean. Earth and Planetary Science Letters, 49, 528-550.

Dehairs, F., Fagel, N., Antia, A.N., Peinert, R., Elskens, M., Goeyens, L., 2000. Export production in the Gulf of Biscay as estimated from barium-barite in settling material: A comparison with new production. Deep-Sea Research I, 47, 583-601.

Dehairs, F., Goeyens, L., Stroobants, N., Bernard, P., Goyet, C., Poisson, A. Chesselet, R., 1990. On suspended barite and the oxygen minimum in the Southern Ocean. Global Biogeochemical Cycles, 4, 85-102.

Dehairs, F., Shopova, D., Ober, S., Veth, C., Goeyens, L., 1997. Particulate barium stocks and oxygen consumption in the Southern Ocean mesopelagic water column during spring and early summer: relationship with export production. Deep-Sea Research II, 44 (1-2), 497-516.

Dehairs, F., Stroobants, N., Goeyens, L., 1991. Suspended barite as a tracer of biological activity in the Southern Ocean. Marine Chemistry, 35: 399-410.

del Giorgio, P.A., Cole, J.J., 2000. Bacterial energetics and growth efficiency. In: D.L. Kirchman (ed.), Microbial Ecology of the Oceans. Wiley & Sons, pp 289-325.

Ducklow, H., 2000. Bacterial production and biomass in the oceans. In: D.L. Kirchman (ed.), Microbial Ecology of the Oceans. Wiley & Sons, pp 85-152.

Eardly, D.F., Carton, M.W., Gallagher, J.M., Patching, J.W., 2001. Bacterial abundance and activity in deep-sea sediments from the eastern North Atlantic. Progress in Oceanography, **50:** 245-259.

Elskens, M., Baeyens, W., Boyd, P., Brion, N., Buesseler K., Dehairs, F., Silver, M., Van Mooy, B., Primary, new and export productions in the NW Pacific during the Vertigo K2 experiments, this issue.

Freydier, R., Dupré, B., Polve, M., 1995. Analyses by Inductively-Coupled Plasma-Mass Spectrometry of Ba Concentrations in Water and Rock Samples - Comparison between Isotope-Dilution and External Calibration with or without Internal Standard. European Mass Spectrometry, 1(3): 283-291.

Fuhrmann, J.A., Azam, F., 1982. Thymidine incorporation as a mesure of heterotrophic bacterioplankton production in marine surface waters: Evaluation and field results, Marine Biology, 66, 109-130.

Ganeshram, R.S., François, R., Commeau, J., Brown-Leger, S.L., 2003. An experimental investigation of barite formation in seawater, Geochimica et Cosmochimica Acta, 67, 2599-2605.

Gonzalèz-Muñoz, M.T., Fernández-Luque, B., Martinez-Ruiz, F., Ben Chekroun, K., Arias, J.M., Rodriguez-Gallego, M., Martinez-Cañamero, M., de Linares, C., Paytan, A., 2003. Precipitation of barite by *Myxococcus xanthus*: Possible implications for the biogeochemical cycle of barium. Applied and Environmental Microbiology, 69 (9), 5722-5725.

Honda, M.C., 2003. Biological pump in the northwestern North Pacific. Journal of Oceanography, 59, 671-684.

Honda, M.C., Kawakami, H., Sasaoka, K., Watanabe, S., Dickey, T., 2006. Quick transport of primary produced organic carbon to the ocean interior. Geophysical Research Letters, 33, doi:101029/2006GL026466.

Jacquet, S.H.M., Dehairs, F., Cardinal, D., Navez, J., Delille, B., 2005. Barium distribution across the Southern Ocean Frontal system in the Crozet-Kerguelen Basin. Marine Chemistry, 95 (3-4): 149-162.

Jacquet, S.H.M., Dehairs, F., Rintoul S., 2004. A high resolution transect of dissolved barium in the Southern Ocean. Geophysical Research Letters, 31, L14301, doi: 10,1029/2004GL20016.

Jacquet, S.H.M., Dehairs, F., Savoye, N., Elskens, M., Cardinal, D., 2007a. Barium cycling along WOCE SR3 line in the Southern Ocean. Marine Chemistry, 106, 33-45.

Jacquet, S.H.M., Dehairs, F., Savoye, N., Obernosterer, I., Christaki, U., Monnin, C., Cardinal, D., Mesopelagic organic carbon mineralization in the Kerguelen Plateau region tracked by biogenic particulate Ba. Deep-Sea Research Part II, in press.

Jacquet, S.H.M., Henjes, J., Dehairs, F., Worobiec, A., Savoye, N., Cardinal, D., 2007b. Particulate Ba-barite and acantharians in the Southern Ocean during the European Iron Fertilization Experiment (EIFEX). Journal of Geophysical Research, Biogeosciences, 112, G04006, doi:10.1029/2006JG000394.

Karl, D.M., Christian, J.R., Dore, J.E., Hebel, D.V., Letelier, R.M., Tupas, L.M., Winn, C.D., 1996. Seasonal and inter-annual variability in primary production and particle flux at station ALOHA. Deep-Sea Research II, 43, 539-568.

Karl, D.M., Lukas, R., 1996. The Hawaii Ocean Time-series (HOT) program: Background, rationale and field implementation. Deep-Sea Research II, 43, 129-156.

Klinkenberg, H., VanBorm W., Souren, F., 1996. A theoretical adaptation of the classical isotope dilution technique for practical routine analytical determinations by means of inductively coupled plasma mass spectrometry. Spectrochimica Acta Part B-Atomic Spectroscopy, 51(1): 139-153.

Klinkhammer G.P., Chan, L.H., 1990. Determination of Barium in Marine Waters by Isotope-Dilution Inductively Coupled Plasma Mass-Spectrometry. Analytica Chimica Acta, 232(2): 323-329.

Kopczynska, E.E., Dehairs, F., Elskens, M., Wright, S., 2001. Phytoplankton variability between the subtropical and Polar Fronts south off Australia: Thriving under regenerative and new production in late summer. Journal of Geophysical Research, 106, 31597-31609.

Kryc K.A., R.W. Murray, D.W. Murray, Al-to-oxide and Ti-to-organic linkages in biogenic sediment: relationships to paleo-export production and bulk Al/Ti, 2003. Earth and Planetary Science Letters, 211, 125-141.

Lam, P.J. and J.K.B. Bishop, 2007. High biomass low export regimes in the Southern Ocean, Deep-Sea Research, II, 54, 601-638.

Lam, P.J, Bishop, J.K.B., Is dust iron supply to the open ocean overblown? Submitted to Geophysical Research Letters.

Lamborg, C.H., Buesseler, K.O., Valdes J., Bertrand, C.H., Manganini S., Pike S., Steinberg D., Trull T., Wilson S., The flux of major, minor and trace elements associated with sinking particles in the mesopelagic "Twilight Zone" of the Northwest and North Central Pacific Ocean, this issue.

Lampitt, R.S., Wishner, K.E., Turley, C.M., Angel, M.V., 1993. Marine snow studies in the Northeast Atlantic Ocean: distribution, composition and role as a food source for migrating plankton, Marine Biology, 116, 689-702.

Lea D. and E. Boyle, 1989. Barium content of benthic foraminifera controlled by bottom-water composition, Nature, 338, 751-753.

Martin, J.H., Knauer, G.A., Karl, D.M., Broenkow, W.W., 1987. VERTEX: carbon cycling in the north-east Pacific. Deep-Sea Research, 34, 267-285.

Monnin, C., Jeandel, C., Cattaldo, T., Dehairs F., 1999. The marine barite saturation state of the world's oceans. Marine Chemistry, 65, 253-261.

Monnin, C., Cividini, D., 2006. The saturation state of the world's ocean with respect to (Ba,Sr)SO_4 solid solutions. Geochimica et Cosmochimica Acta, 70, 3290-3298.

Murray, R. W., Leinen, M., 1996. Scavenged excess aluminum and its relationship to bulk titanium in biogenic sediment from the central equatorial Pacific Ocean, Geochimica et Cosmochimica Acta, 60,3869-3878.

Nagata, T., Fukuda H., Fukuda R., Koike I., 2000. Bacterioplankton distribution and production in deep Pacific waters: Large-scale geographic variations and possible coupling with sinking particle fluxes. Limnology and Oceanography, 45, 426-435.

Nishioka, J., Ono, T., Saito, H., Nakatsuka, T., Takeda, S., Yoshimura, T., Suzuki, K., Kuma, Nakabayashi, K., Tsumune, S.D., Mitsudera, H., Johnson, W.K., Tsuda, A., 2007. Iron supply to the western subarctic Pacific: Importance of iron export from the Sea of Okhotsk, Journal of Geophysical Research - Oceans, 112, C10012, doi:10.1029/2006JC004055.

Passow, U., Shipe, R.F., Murray, A., Pak, D.K., Brzezinski, M.A., Alldredge, A.L., 2001. The origin of transparent exopolymer particles (TEP) and their role in the sedimentation of particulate matter, Continental Shelf Research, 21, 327-346.

Peterson M.L., Wakeham S.G., Lee C., Askea M.A.and Miquel J.C., 2005**.** Novel techniques for collection of sinking particles in the ocean and determining their settling rates, Limnology and Oceanography: Methods, 3, 520-532.

Pike, S., Andrews, J., Trull, T., Buesseler, K.O., 2006. A high resolution study of particle export using Thorium-234 in the N. Central Pacific and NW Pacific as part of the VERTIGO project, 2006 Ocean Sciences Meeting, Honolulu, Hawaii.

Reinthaler, T., Van Aken, H., Veth, C., Arístegui, J., Robinson, C., Williams P. J. L. B., 2006. Prokaryotic respiration and production in the meso- and bathypelagic realm of the eastern and western North Atlantic basin. Limnology and Oceanography, 51, 1262-1273.

Reitz A., Pfeifer, K., de Lange, G.J., Klump, J., 2004. Biogenic barium and the detrital Ba/Al ratio: a comparison of their direct and indirect determination. Marine Geology, 204, 289-300.

Robin, E., Rabouille, C., Martinez, G., Lefevre, I., Reyss, J.L., van Beek, P., Jeandel, C., 2003. Direct barite determination using SEM/EDS-ACC system: implication

for constraining barium carriers and barite preservation in marine sediments, Marine Chemistry, 82, 289-306.

Saito, H., Tsuda A., Kasai H., 2002. Nutrient and plankton dynamics in the Oyashio region of the western subarctic Pacific Ocean, Deep-Sea Research II, 49, 5463-5486.

Shopova, D., Dehairs, F., Baeyens, W., 1995. A simple model of biogeochemical element distribution in the water column of the Southern Ocean. Journal of Marine Systems, 6, 331-344.

Silver, M.W., Coale, S.L., Smith, S., Tanner, S., Gibson, A., 2006. Primary Producers at VERTIGO Study Sites: The Phytoplankton Community During ALOHA and K2 Deployments, 2006 Ocean Sciences meeting, Honolulu, Hawaii.

Stanley, R.H.R., Buesseler, K.O., Manganini, S.J., Steinberg, D.K., Valdes, J.R., 2004. A comparison of major and minor elemental fluxes collected in neutrally buoyant and surface-tethered sediment traps. Deep-Sea Research I, 51, 1387-1395.

Steinberg, D.K., Van Mooy, B.A.S., Buesseler, K.O., Boyd, P.W., Kobari T., Karl, D.M., Microbial vs. zooplankton control of sinking particle flux in the ocean's twilight zone. Limnology and Oceanography, in press.

Sternberg, E., 2005. La Barytine, Traceur en Paleocéanographie, Thèse de doctorat, Université Paul Sabatier, Toulouse.

Stroobants, N., Dehairs, F., Goeyens, L., Vanderheijden, N., Van Grieken R., 1991. Barite formation in the Southern Ocean water column. Marine Chemistry, 35, 411-421.

Tamburini, C., Garcin, J., Bianchi, A., 2003. Role of deep-sea bacteria in organic matter mineralization and adaptation to hydrostatic pressure conditions in the NW Mediterranean Sea. Aquatic Microbial Ecology, 32, 209-218.

Tamburini, C., Garcin, J., Ragot, M., Bianchi, A., 2002. Biopolymer hydrolysis and bacterial production under ambient hydrostatic pressure through a 2000m water column in the NW Mediterranean. Deep Sea Research II, 49**,** 2109-2123.

Taylor, S.R., McLennan, S.M., 1985. The continental crust: its composition and evolution. Blackwell Scientific Publications, 312pp.

Tazaki, K., Webster, J., Fyfe, W.S., 1997. Transformation processes of microbial barite to sediments in Antarctica. Journal of the Mineralogical Society, 26, 63-68.

Tomczak M. and J.S. Godfrey, 1994. Regional Oceanography: An Introduction, Pergamon Press, 422pp.

Turley, C. M., Dixon, J. L., 2002. Bacterial numbers and growth in surficial deep-sea sediments and phytodetritus in the NE Atlantic: Relationships with particulate organic carbon and nitrogen. Deep Sea Research I, 49, 815-826.

Trull, T., Buesseler, K., Bray, S., Moy, C., Ebersbach, F., Lamborg,C., Pike, S., Manganini, S., In-situ particle sinking rates in mesopelagic depths from the Sub-Arctic Pacific, this issue.

van Beek P., R. François, M. Conte, J.-L. Reyss, M. Souhaut and M. Charrette, 2007. $^{228}Ra/^{226}Ra$ and $^{226}Ra/Ba$ ratios to track barite formation and transport in the water column, Geochimica et Cosmochimica Acta, 71, 71-86.

Webb, D. J., Killworth, P. D., Coward, A. C., Thomson, S. R., 1991. The FRAM Atlas of the Southern Ocean. Natural Environment Research Council, Swindon, Archway Press, 67 pp.

Webster, R.K., 1960. Methods in Geochemistry, in: Smales, A.A., Wager, L.R. (Eds), Interscience, New York, pp202-246.

Wilson, S. E., Steinberg, D. K., Buesseler, K. O., 2007. Changes in fecal pellet characteristics with depth as indicators of zooplankton repackaging of particles in the mesopelagic zone, this issue.

Table 1: Comparison between carbon respiration by bacteria and zooplankton (data from Steinberg et al., in press) and POC remineralization based on Ba_{xs} over the 150 to 500m depth region; the comparison between bacterial respiration - mesopelagic Ba_{xs} content is based on casts taken within a day's interval; min., max. bacterial respiration values calculated considering TdR conversion factors 1 and 2 x 10^{18} cells mol^{-1} and BGE values of 0.15 and 0.10, respectively (see methods section); (n) = number of casts.

SITE Julian day	Bacterial Respiration[1] mgC m^{-2} d^{-1} min. – max.	Zooplankton Respiration[1] mgC m^{-2} d^{-1}	Mesopelagic Ba_{xs} pM min. – max.	POC remineralization from Ba_{xs}[2] mgC m^{-2} d^{-1} min. – max.
ALOHA 177 - 191	16 – 55 (2)	6.2 - 6.7	157 – 205 (5)	12 – 36 * (5)
K2 219 - 226	46 – 147 (2)	27.1	367 – 713 (3)	33 – 106 ** (3)

[1] data from Steinberg et al. (in press)

[2] calculated using Ba_{xs} values in 4th column and eqs. (1) & (2); the average standard error on these values is 22%

* residual Ba_{xs} taken as 90 and 0 pM for minimum and maximum, resp. (see text)

** residual Ba_{xs} taken as 180 and 90 pM for minimum and maximum, resp. (see text)

Table 2: Comparison of POC remineralization between 150 and 500m based on mesopelagic Ba_{xs} with NBST POC flux decrease (ΔPOC flux = POC flux at 500m – POC flux at 150m) and New Production (all fluxes in mgC m^{-2} d^{-1}); POC remineralization based on Ba_{xs} was calculated using eqs. (1 & 2); several CTD casts were obtained during each of the NBST deployments and Ba_{xs} contents, as well as POC remineralization values based on Ba_{xs} represent minima – maxima; (n) = number of casts sampled per corresponding NBST deployment.

SITE Event Julian day	NBST POC flux[1] mgC m^{-2} d^{-1} 150m 300m 500m	NBST ΔPOC flux[1] (150-500m) mgC m^{-2} d^{-1}	Mesopelagic Ba_{xs} (150-500) pM min. – max.	POC reminer. based on Ba_{xs}[2] (150-500m) mgC m^{-2} d^{-1} min. – max.	New Production[3] mgC m^{-2} d^{-1}
ALOHA NBST #1 d. 177 - 182	18 7.2 3.6	14.4	193 - 205 (2)	18 - 36* (2)	30
ALOHA NBST #2 d. 186 - 191	18 6.0 3.6	14.4	157 - 172 (3)	12 - 30* (3)	30
K2 NBST #1 d. 209 - 215	62 47 27	33	227 - 303 (3)	8 - 38** (3)	151
K2 NBST #2 d. 219 - 226	23 17 13	10	367 - 713 (3)	33 - 106 ** (3)	72

[1] NBST POC flux data are from Buesseler et al. (2007)

[2] calculated using eqs. (1) and (2)

[3] new production data are from Elskens et al. (this volume and unpublished results)

* residual Ba_{xs} taken as 90 and 0 pM for minimum and maximum, resp. (see text)

** residual Ba_{xs} taken as 180 and 90 pM for minimum and maximum, resp. (see text)

Figure captions

Figure 1: Stations ALOHA and K2; temperature – salinity plots (A); dissolved O_2 profiles (µmol l^{-1}) (B); temperature profiles in the upper 100m (C, D; cast number indicated); arrows in A and B indicate cast 50 at K2 showing an offset in temperature and dissolved O_2.

Figure 2: Station K2; profiles of particulate Al (A, B; nmol l^{-1}) and Ba_{xs} (C, D; pmol l^{-1}); A, C: during NBST deployment #1 (Julian day 209-215), B, D: during NBST deployment #2 (Julian day 219-226).

Figure 3: (A) Average profiles of Ba_{xs} (pmol l^{-1}) at ALOHA and K2 sites shown together with a particulate ^{234}Th profile (dpm l^{-1}; the latter data from Buesseler et al., in preparation); (B) average profiles for total Sr; ALOHA: 5 CTD casts; K2: 6 CTD casts; error bars are 1 s.d. and plotted in negative or positive direction only for clarity.

Figure 4: Column integrated (0-1000m) bacterial production (mgC m^{-2} d^{-1}) at stations ALOHA (open triangles, Julian day 177; closed triangles, Julian Day 187) and K2 (closed squares, Julian Day 222; open squares, Julian day 226); data from Steinberg et al. (in press).

Figure 5: Relationship between column integrated (150 to 500m) bacterial production (mgC m^{-2} d^{-1}) and depth weighted average Ba_{xs} contents (pmol l^{-1}) in the same depth interval (r^2 = 0.84; $p<0.1$); error bars indicate ranges of values; circles: ALOHA; squares: K2.

Figure 6: Average profiles of dissolved Ba (nmol l^{-1}) and saturation index (Ω) for pure $BaSO_4$ (closed symbols) and $(Ba,Sr)SO_4$ solid solution; (A) ALOHA; (B) K2; error bars = 1 s.d.

Figure 1

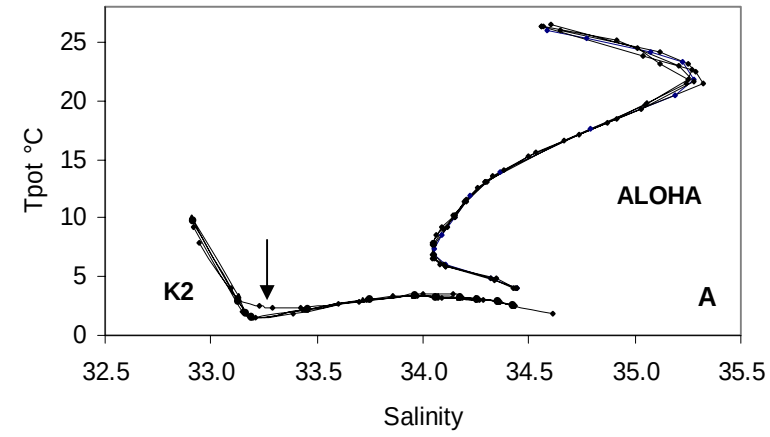
Tpot °C
25
20
15
10
5
0
32.5
33.0
33.5
34.0
34.5
35.0
35.5
Salinity
K2
ALOHA
A

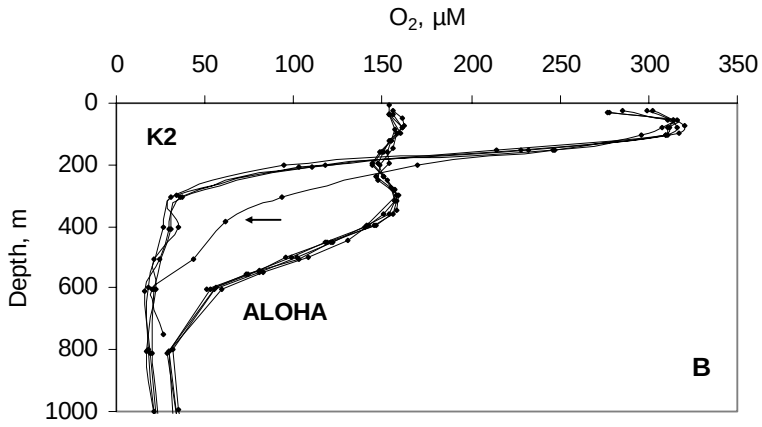
O2, µM
0
50
100
150
200
250
300
350
Depth, m
0
200
400
600
800
1000
K2
ALOHA
B

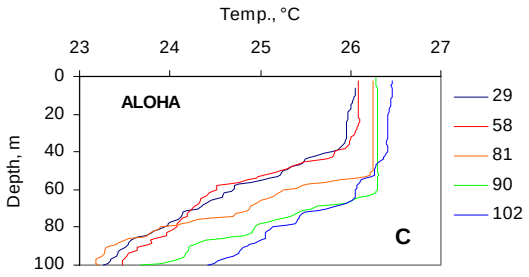
Temp., °C
23
24
25
26
27
Depth, m
0
20
40
60
80
100
ALOHA
C
29
58
81
90
102

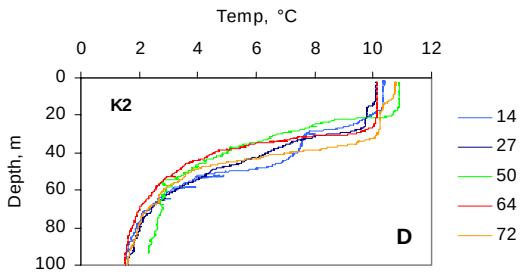
Temp, °C
0
2
4
6
8
10
12
Depth, m
0
20
40
60
80
100
K2
D
14
27
50
64
72

1

2 Figure 2

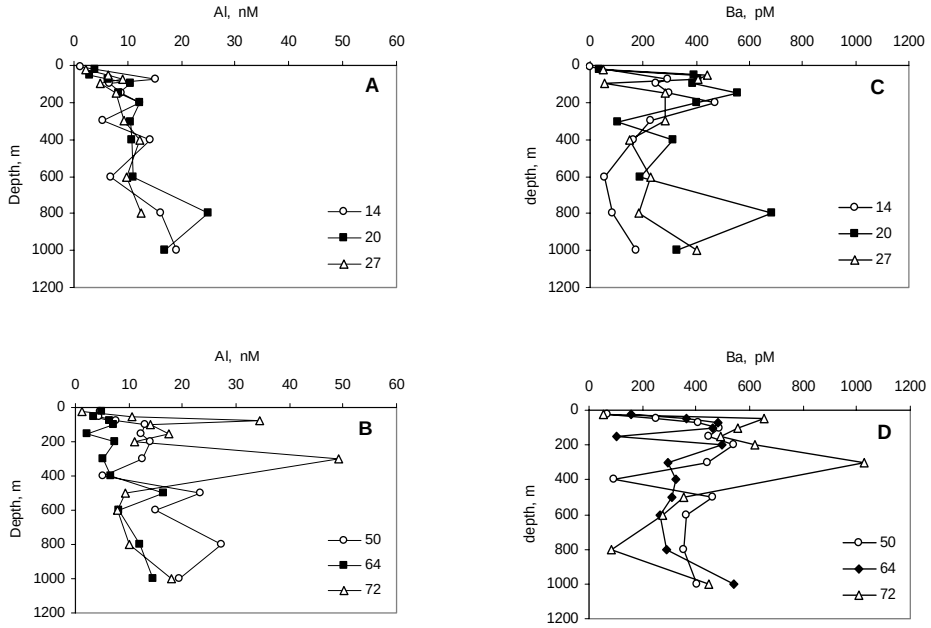
Al, nM
Depth, m
A
14
20
27
Ba, pM
depth, m
C
Al, nM
Depth, m
B
50
64
72
Ba, pM
depth, m
D

3

4 Figure 3

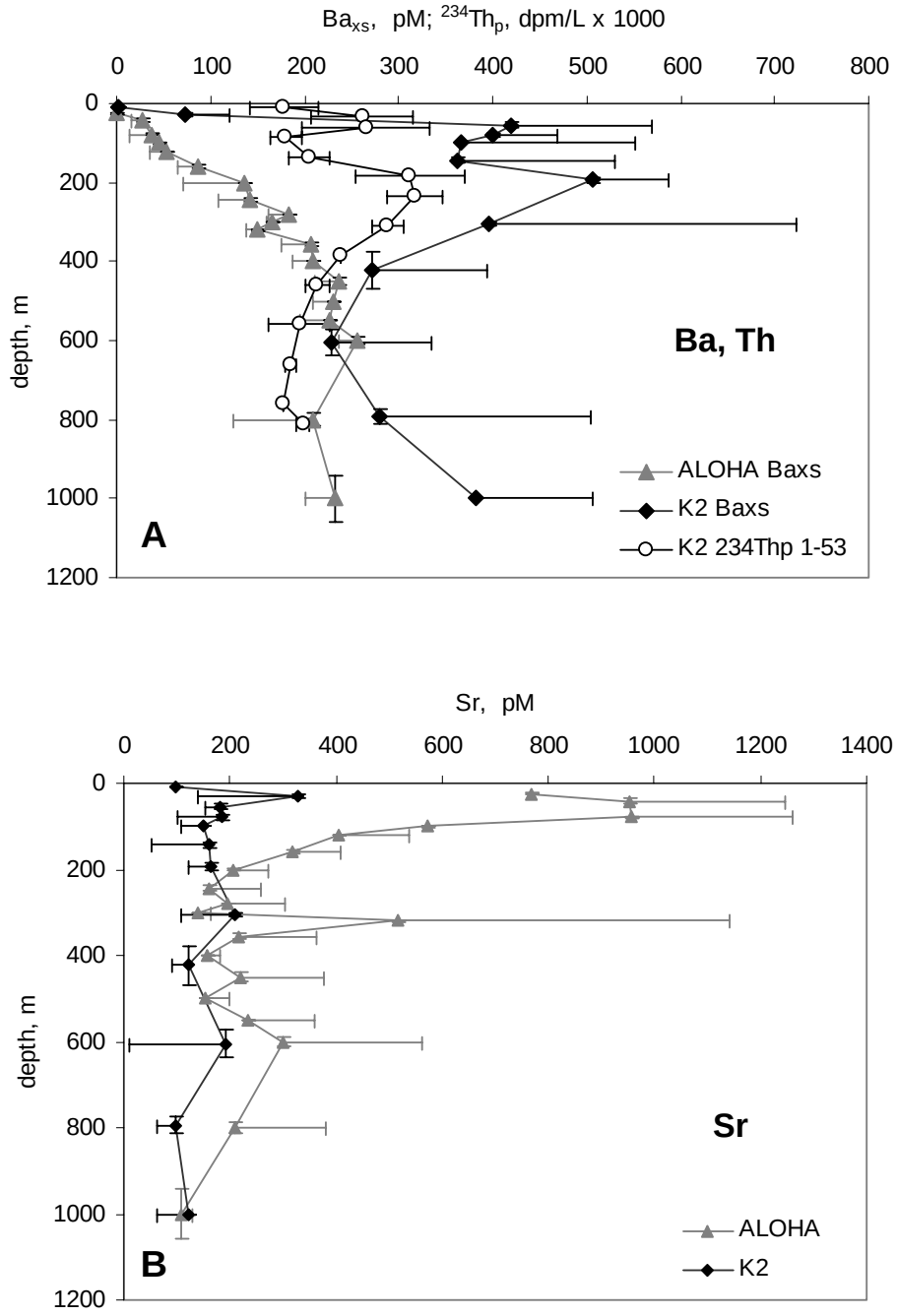
Ba$_{xs}$, pM; ^{234}Th$_p$, dpm/L x 1000
0
100
200
300
400
500
600
700
800
depth, m
0
200
400
600
800
1000
1200
Ba, Th
ALOHA Baxs
K2 Baxs
K2 234Thp 1-53
A
Sr, pM
0
200
400
600
800
1000
1200
1400
depth, m
0
200
400
600
800
1000
1200
Sr
ALOHA
K2
B

5

Figure 4

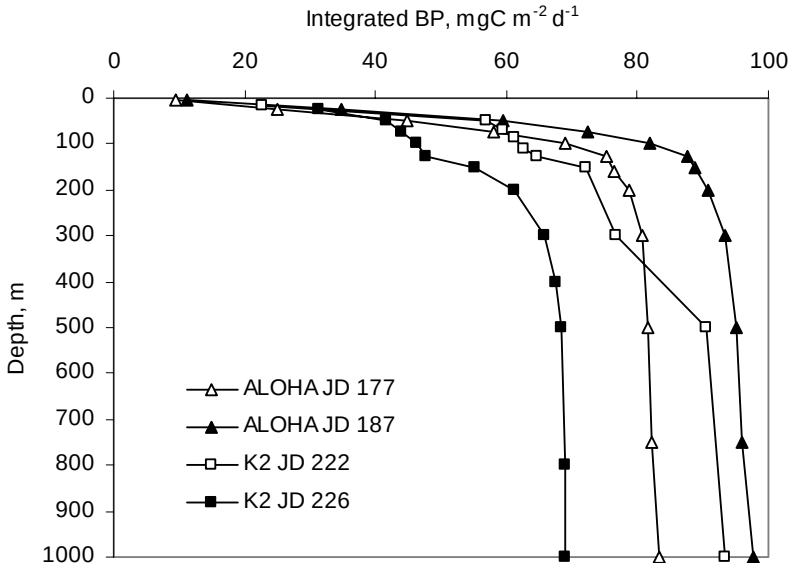
Integrated BP, mgC m-2 d-1
0
20
40
60
80
100
Depth, m
0
100
200
300
400
500
600
700
800
900
1000
ALOHA JD 177
ALOHA JD 187
K2 JD 222
K2 JD 226

Figure 5

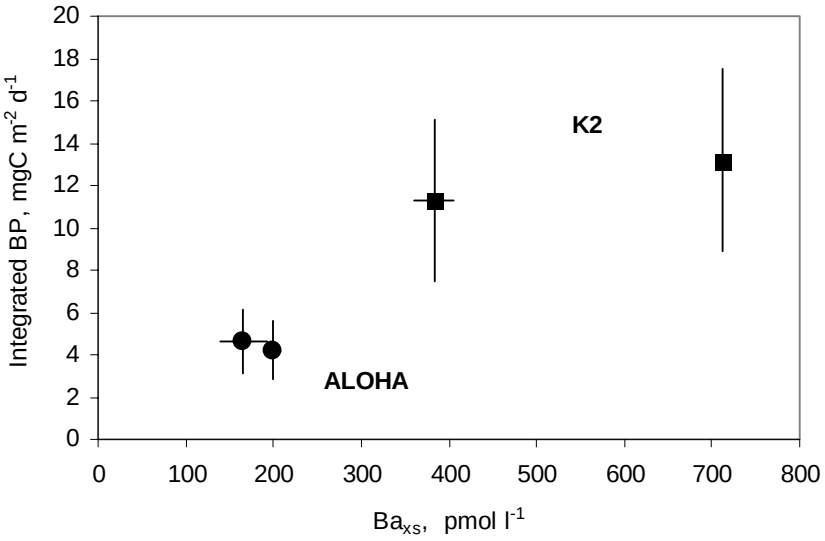
Integrated BP, mgC m-2 d-1
Bacs, pmol l-1
K2
ALOHA
0
2
4
6
8
10
12
14
16
18
20
0
100
200
300
400
500
600
700
800

14 Figure 6

15

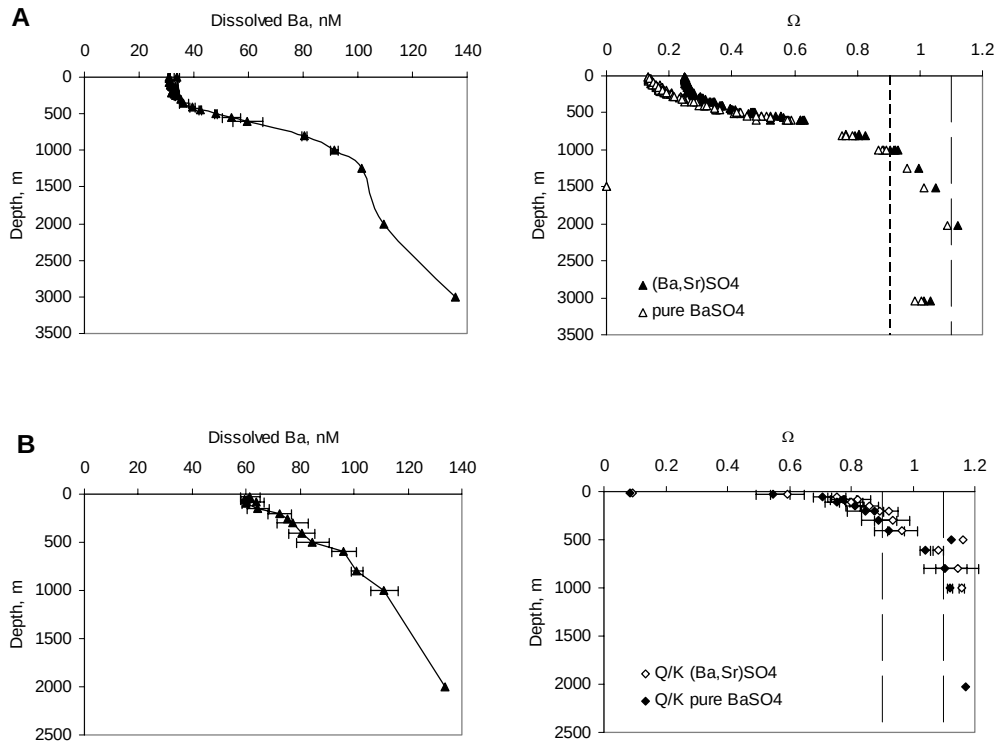

16
17
18
19
20
21